Supplementary Information for

A Water-stable Terbium−MOF Sensor for Selective, Sensitive, and Recyclable Detection of Al^{3+} and CO_3^{2-} Ions

Zhiying Zhan†, Yuejiao Jia†, Donghua Li, Xiaolei Zhang, Ming Hu*

(Inner Mongolia Key Laboratory of Chemistry and Physics of Rare Earth Materials; School of Chemistry and Chemical Engineering, Inner Mongolia University, Hohhot 010021, China)

Tel.: +86-471-4992981 .E-mail addresses:hm988@126.com

Table S1. The selected bond lengths [Å] and angles [°] for **1**.

Compound **1**			
Tb(1)-O(1)	2.378(5)	Tb(1)-O(2)#2	2.437(5)
Tb(1)-O(9)	2.383(6)	Tb(1)-O(4)#3	2.453(5)
Tb(1)-O(8)	2.383(5)	Tb(1)-O(3)#3	2.453(5)
Tb(1)-O(7)#1	2.422(5)	Tb(1)-O(1)#2	2.613(5)
Tb(1)-O(6)	2.423(5)		
O(1)-Tb(1)-O(9)	85.2(2)	O(7)#1-Tb(1)-O(4)#3	123.32(19)
O(1)-Tb(1)-O(8)	74.50(18)	O(6)-Tb(1)-O(4)#3	72.5(2)
O(9)-Tb(1)-O(8)	77.8(2)	O(2)#2-Tb(1)-O(4)#3	131.38(19)
O(1)-Tb(1)-O(7)#1	140.64(18)	O(1)-Tb(1)-O(3)#3	80.17(18)
O(9)-Tb(1)-O(7)#1	74.5(2)	O(9)-Tb(1)-O(3)#3	126.13(18)
O(8)-Tb(1)-O(7)#1	68.52(18)	O(8)-Tb(1)-O(3)#3	143.42(18)
O(1)-Tb(1)-O(6)	150.78(18)	O(7)#1-Tb(1)-O(3)#3	138.86(18)
O(9)-Tb(1)-O(6)	96.8(2)	O(6)-Tb(1)-O(3)#3	75.16(17)
O(8)-Tb(1)-O(6)	134.52(18)	O(2)#2-Tb(1)-O(3)#3	82.73(17)
O(7)#1-Tb(1)-O(6)	66.58(17)	O(4)#3-Tb(1)-O(3)#3	53.35(17)
O(1)-Tb(1)-O(2)#2	115.07(17)	O(1)-Tb(1)-O(1)#2	64.4(2)
O(9)-Tb(1)-O(2)#2	148.54(19)	O(9)-Tb(1)-O(1)#2	140.8(2)
O(8)-Tb(1)-O(2)#2	84.6(2)	O(8)-Tb(1)-O(1)#2	70.85(18)
O(7)#1-Tb(1)-O(2)#2	74.84(19)	O(7)#1-Tb(1)-O(1)#2	113.37(17)
O(6)-Tb(1)-O(2)#2	77.27(19)	O(6)-Tb(1)-O(1)#2	121.95(19)
O(1)-Tb(1)-O(4)#3	80.28(19)	O(2)#2-Tb(1)-O(1)#2	50.71(17)
O(9)-Tb(1)-O(4)#3	73.21(19)	O(4)#3-Tb(1)-O(1)#2	121.20(17)
O(8)-Tb(1)-O(4)#3	142.8(2)	O(3)#3-Tb(1)-O(1)#2	74.57(16)

Symmetry transformations used to generate equivalent atoms: #1 -x+3,-y+1,-z #2 -x+2,-y,-z #3 x+1,y,z

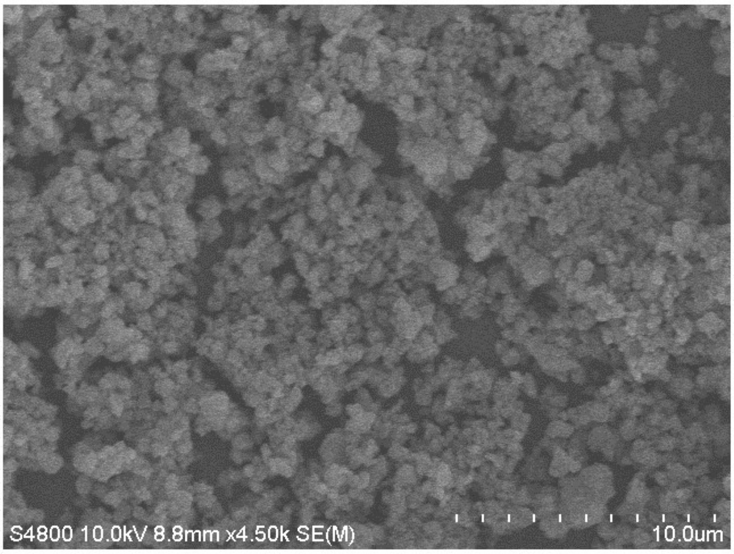

Fig. S1 The SEM image of **1** after grounding**.**

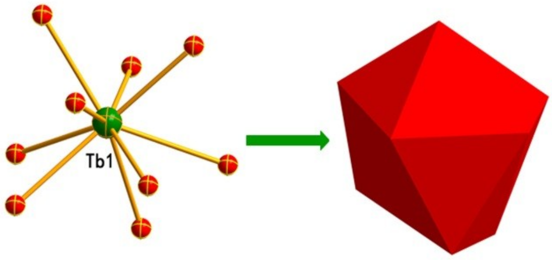

Fig. S2 The monocapped square antiprism coordination geometry of Tb^{3+} ion.

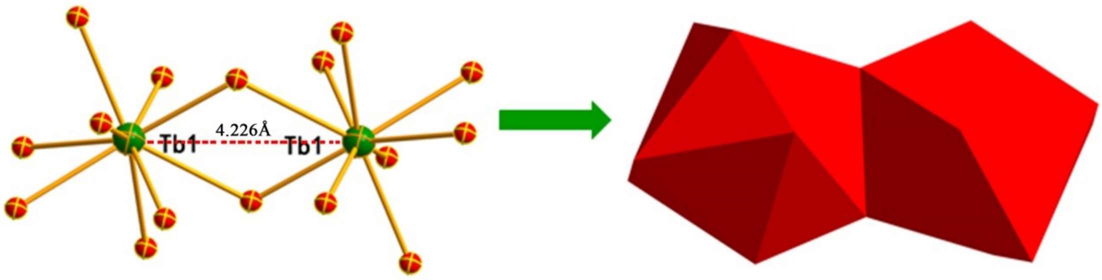

Fig. S3 The binuclear constituted by Tb^{3+} ions.

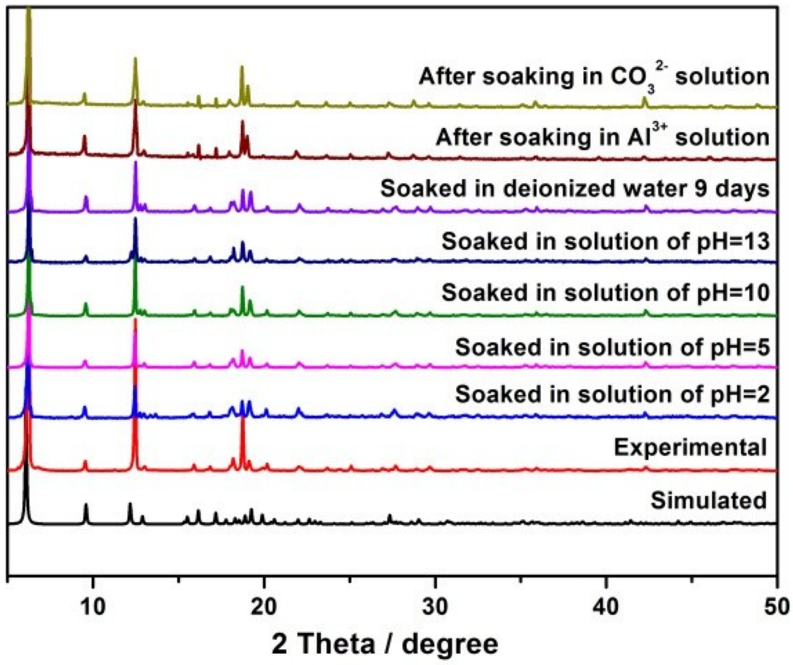

Fig. S4 PXRD patterns of compound **1** simulated from the X-ray single-crystal structure, as-synthesized samples of compound **1**, compound **1** soaked in various solutions**,** and power X-ray diffraction patterns of **1** after five recyclable experiments.

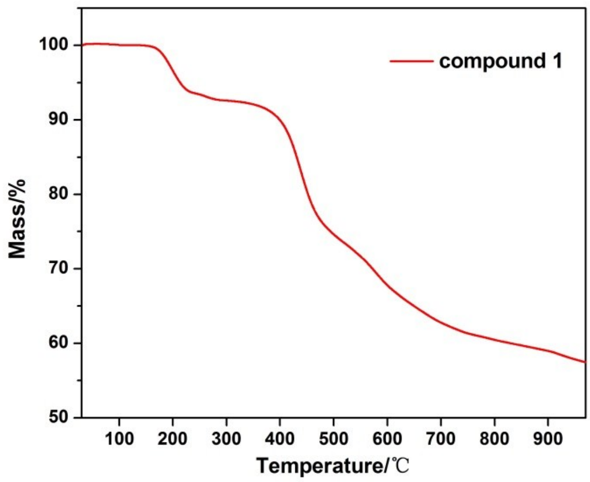

Fig. S5 View of the TG analysis profile of compound **1**.

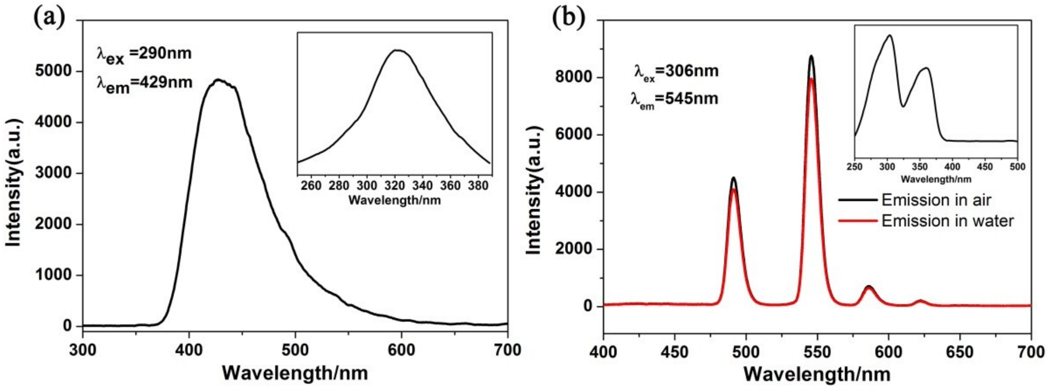

Fig. S6 (a) The emission spectrum of H_2ppda ligand. Insets: The excitation spectrum of H_2ppda ligand; (b) The emission spectra of compound **1** in the solid-state and aqueous suspension, respectively. Insets: The excitation spectrum of compound **1**.

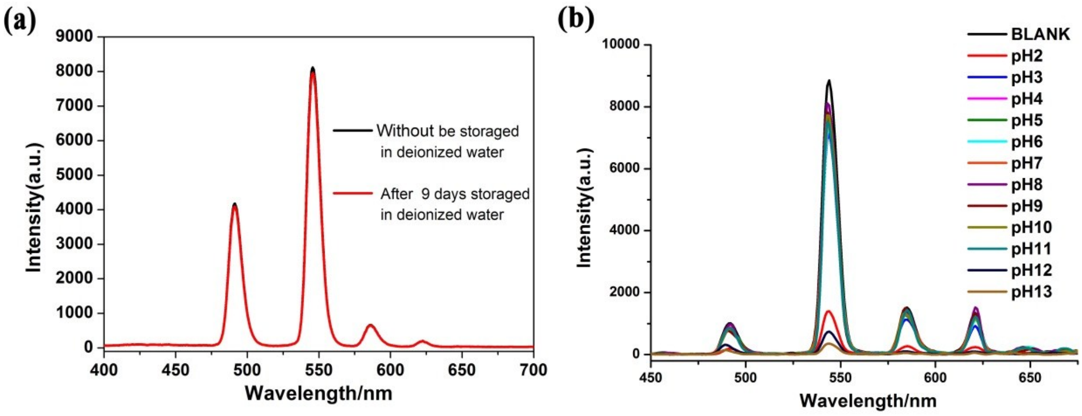

Fig.S7 (a)The emission spectra of **1** without and after 9 days' storage in deionized water; (b)The emission spectra of **1** immersed in acid/base solutions with pH values varied from 2 to 13.

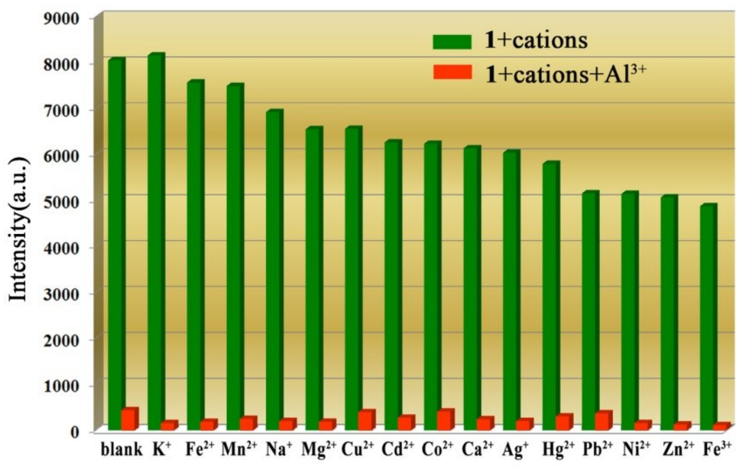

Fig. S8 The fluorescence intensity for **1** exposed to single cation and mixed cations in aqueous solutions.

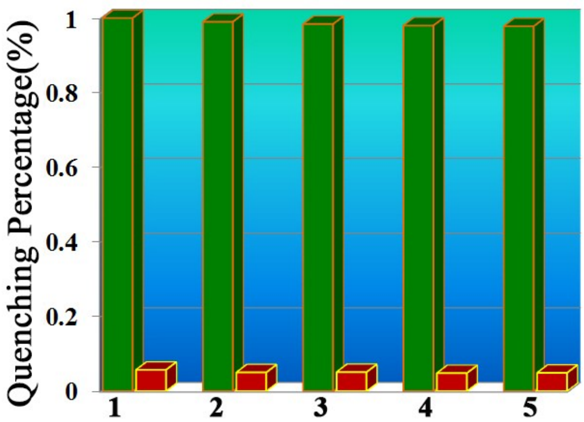

Fig. S9 Quenching and recovery test of **1** in aqueous solution. The green columns represent the initial relative luminescent intensity and the red columns represent the relative intensity on addition of Al^{3+}.

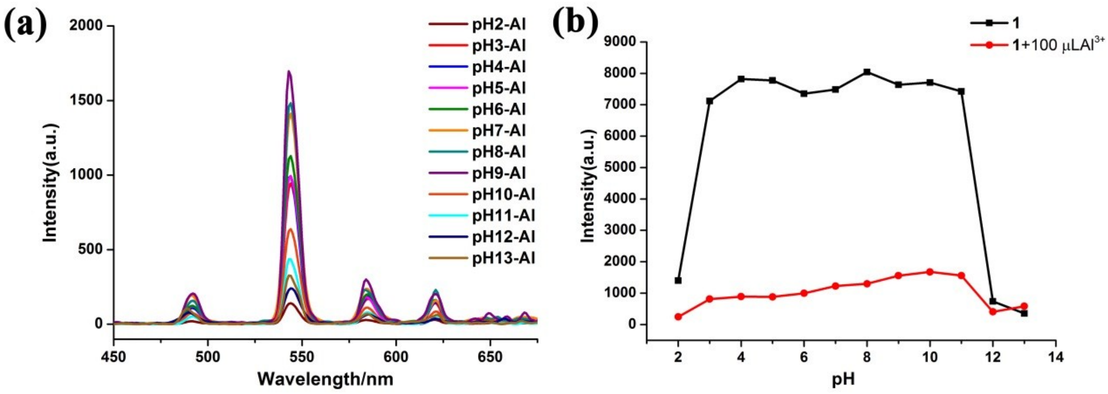

Fig. S10 (a) PL spectra of **1** dispersed in various aqueous solutions (pH 2-13) in presence of 100μL Al^{3+} ion; (b) Comparison of fluorescence intensity for **1** dispersed in aqueous solutions of pH 2-13(black line) and in presence of 100μL Al^{3+} ion (red line).

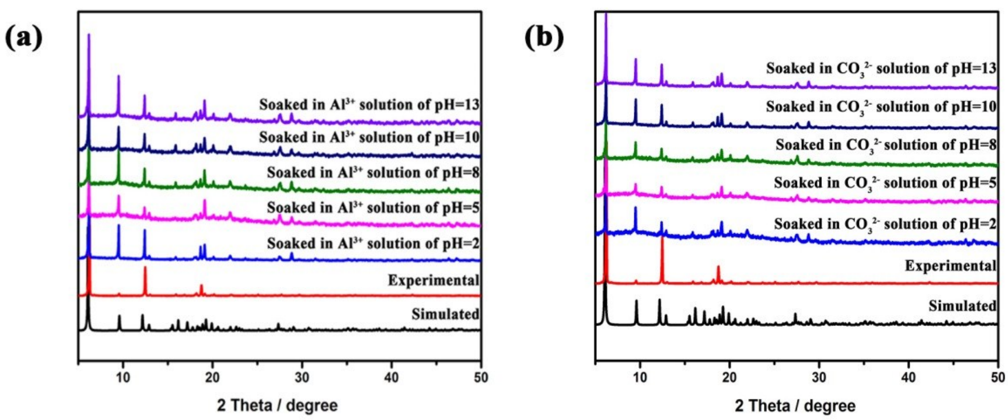

Fig. S11 PXRD patterns of compound **1** simulated from the X-ray single-crystal structure, as-synthesized samples of compound **1**, compound **1** soaked in Al^{3+} (a) and CO_3^{2-} (b) solutions of different pH.

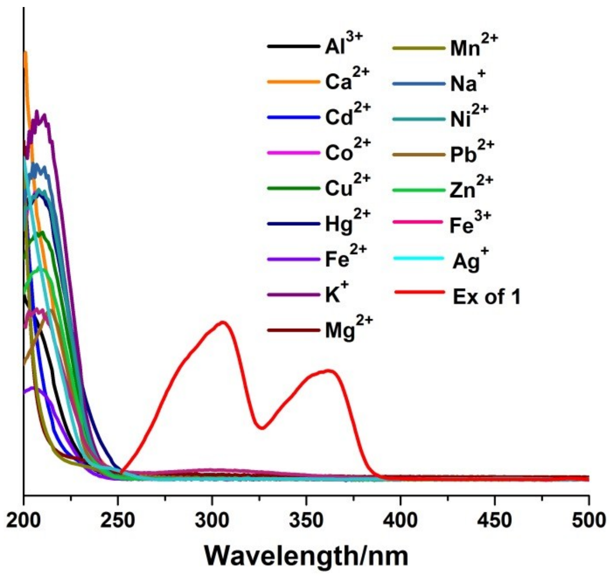

Fig. S12 The UV-Vis adsorption spectra of $M(NO_3)_X$ aqueous solutions and the excitation spectrum of **1**.

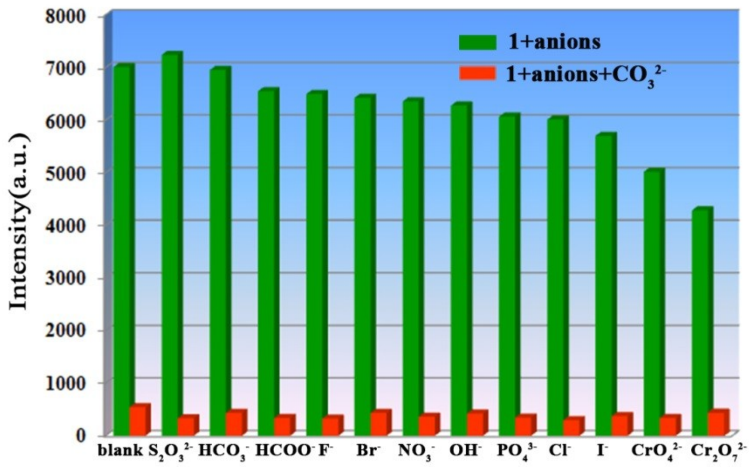

Fig. S13 The fluorescence intensities for **1** exposed to single anion and mixed anions in aqueous solutions.

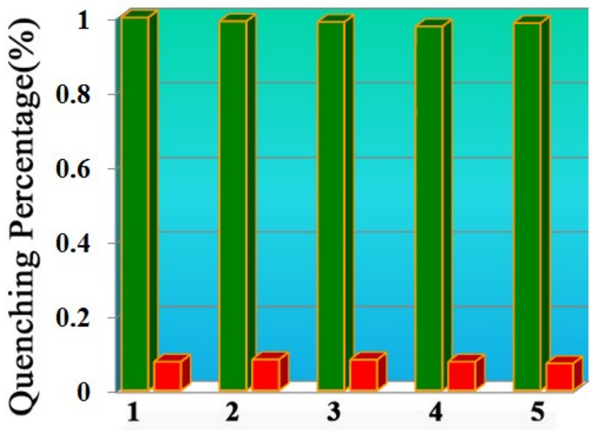

Fig. S14 Quenching and recovery test of **1** in aqueous solution. The green columns represent the initial relative luminescent intensity and the red columns represent the relative intensity on addition of CO_3^{2-}.

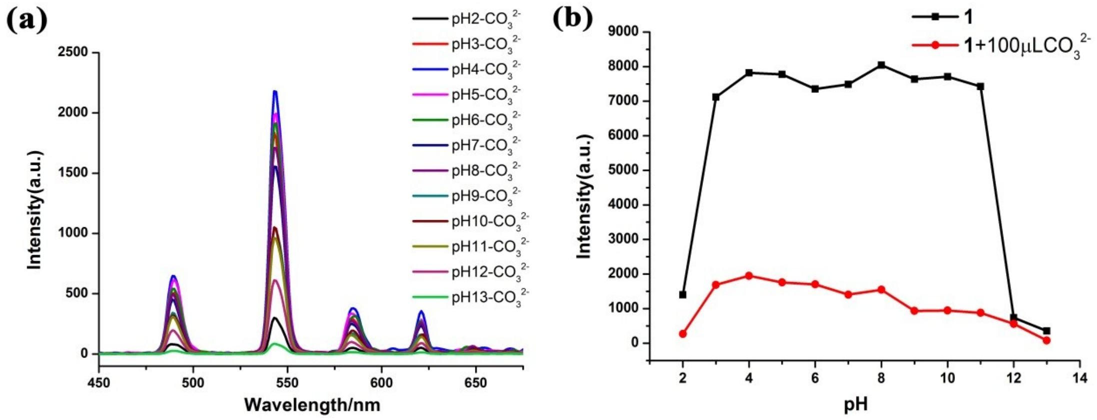

Fig. S15 (a) PL spectra of **1** dispersed in various aqueous solutions of pH = 2-13 in presence of 100 μL CO_3^{2-} ion; (b) Comparison of fluorescence intensity for **1** dispersed in aqueous solutions of pH = 2-13 (black line) and in presence of 100 μL CO_3^{2-} ion (red line).

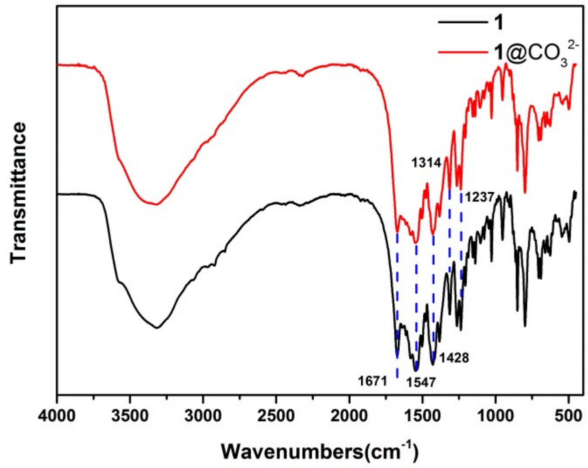

Fig. S16 FT-IR spectra of **1** after immersed in K_2CO_3 aqueous solution and the untreated powder.

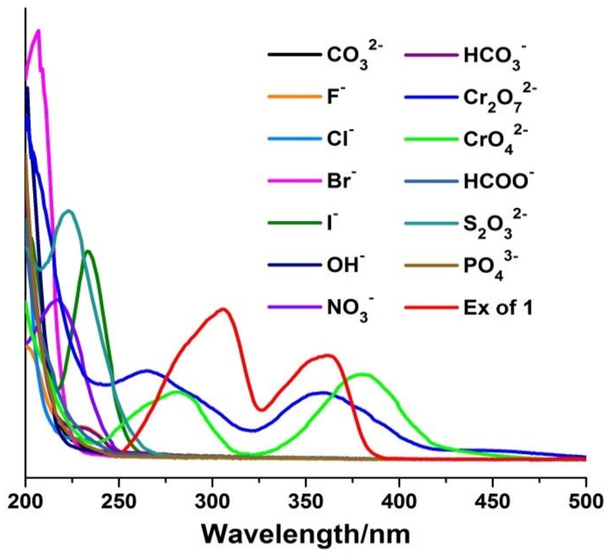

Fig. S17 The UV-Vis adsorption spectra of $K(anion)_x$ aqueous solutions and the excitation spectrum of **1**.

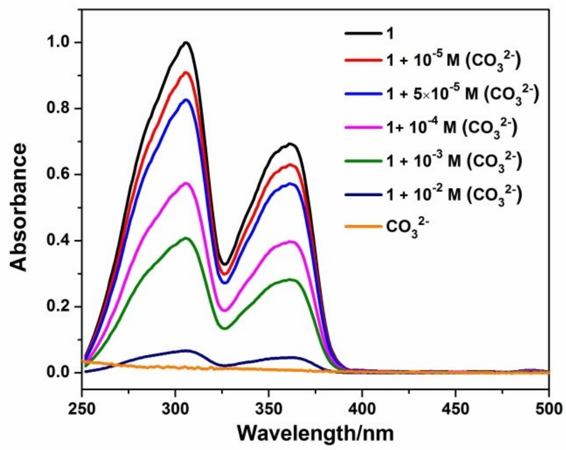

Fig. S18 The UV-Vis adsorption spectra of **1** after adding various concentrations of K_2CO_3 aqueous solutions.

Table S2 Comparison of literature reports for MOFs as sensors of Al^{3+}

MOF	K_{SV} (M^{-1})	Detection Limit	Medium	Ref.
$[Tb(ppda)(ox)_{0.5}(H_2O)_2]_n$ (**1**)	5.26×10^3	5.66×10^{-6} M (152 ppb)	H_2O	**This work**
$[\{Cd_2(syn\text{-}dftpmcp)(1,3\text{-}BDC)_2\}\cdot 0.5DMF\cdot H_2O]_n$	/	183 ppb	CH_3CN	1
UiO-66-NH2-SA	/	6.98 μM	H_2O	2
MOF-LIC-1 (Eu-MOF)	3.79×10^4	/	DMF	3
$[Cd(PAM)(4\text{-}bpdb)_{1.5}]\cdot DMF$ (Cd-MOF)	2.3×10^4	5.6×10^{-7} M	H_2O	4
$\{(Me_2NH_2)[Tb(OBA)_2]\cdot(Hatz)\cdot(H_2O)_{1.5}\}_n$ (**1**)	3.4×10^4	/	H_2O	5
$[Zn_2(HL)_3]^+$@MOF-5	7.478×10^4	/	DMF	6

Table S3 Comparison of literature reports for MOFs as sensors of CO_3^{2-}

MOF	K_{SV} (M^{-1})	Detection Limit	Medium	Ref.
$[Tb(ppda)(ox)_{0.5}(H_2O)_2]_n$ (**1**)	1.78×10^3	3.76×10^{-7} M (0.38 μM)	H_2O	**This work**
$[Eu](Hhpip)_2(OAc)_6]$	9.142×10^3	7.8μM	DMSO	7
$\{[Eu(HL)(H_2O)_3]\cdot H_2O\}_n$(**1**)	3.78×10^3	10^{-6} M	H_2O	8
$[\{[Eu(HBPTC)(H_2O)_2]\cdot 2DMF\}_n]$ film	/	10^{-6} M	H_2O	9
(E)-3-(4-methoxyphenyl)-4-[(4-nitrobenzylidene)-amino]-1H-1,2,4-triazole-5(4H)-thione (**6**)	/	1.91 μM	EtOH/water (3:7, v/v)	10
$\{[Zn_2(\mu_3\text{-}OH)(cpta)(4,4\ \text{-}bipy)]\cdot H_2O\}_n$ (**1**)	9.47×10^3	5.55×10^{-6} M (5.55 μM)	H_2O	11

References

1. W. X. Li, J. H. Gu, H. X. Li, M. Dai, D. J. Young, H. Y. Li and J. P. Lang, *Inorg Chem*, 2018, **57**, 13453-13460.
2. S. Y. Zhu and B. Yan, *Dalton Trans*, 2018, **47**, 1674-1681.
3. J.N. Hao and B. Yan, *J. Mater. Chem. C*, 2014, **2**, 6758-6764.
4. W. Chen, Y. Lin, X. Zhang, N. Xu and P. Cheng, *Inorganic Chemistry Communications*, 2017, **79**, 29-32.
5. D. M. Chen, N. N. Zhang, C. S. Liu and M. Du, *Journal of Materials Chemistry C*, 2017, **5**, 2311-2317.
6. M. M. Wu, J. Y. Wang, R. Sun, C. Zhao, J. P. Zhao, G. B. Che and F. C. Liu, *Inorg Chem*, 2017, **56**, 9555-9562.
7. Y. N. Lu, J. L. Peng, X. Zhou, J. Z. Wu, Y. C. Ou and Y. P. Cai, *CrystEngComm*, 2018, **20**, 7574-7581.
8. H. Wang, J. Qin, C. Huang, Y. Han, W. Xu and H. Hou, *Dalton transactions*, 2016, **45**, 12710-12716.
9. H. Liu, H. Wang, T. Chu, M. Yu and Y. Yang, *J. Mater. Chem. C*, 2014, **2**, 8683-8690.
10. M. Saleem, N. G. Choi and K. H. Lee, *International Journal of Environmental Analytical Chemistry*, 2015, **95**, 592-608.
11. A. Ghorai, J. Mondal, R. Chandra and G. K. Patra, *RSC Advances*, 2016, **6**, 72185-72192.